processes

MDPI

Article

Supercritical Fluid Extraction of Bioactive Compounds from Chamomile Leaves Grown in Tarma, Peru

Larry Oscar Chañi-Paucar [1,*], Joselin Paucarchuco-Soto [1], Diner Mori-Mestanza [2], Grimaldo Wilfredo Quispe Santivañez [1], Walter Javier Cuadrado Campó [1], Perfecto Chagua-Rodríguez [1], Julio Cesar Maceda Santivañez [1,3], Julio Cezar Johner Flores [1], Ádina L. Santana [4] and Maria Angela A. Meireles [5]

[1] Grupo de Investigación en Ingeniería de Alimentos y Agroindustria (GIIAA), Universidad Nacional Autónoma Altoandina de Tarma (UNAAT), Carretera La Florida-Cochayoc, Huancucro 2092, Junin 12651, Peru
[2] Instituto de Investigación, Innovación y Desarrollo para el Sector Agrario y Agroindustrial (IIDAA), Facultad de Ingeniería y Ciencias Agrarias, Universidad Nacional Toribio Rodríguez de Mendoza de Amazonas, Chachapoyas 01000, Peru
[3] Mass Spectrometry and Chemical Ecology Laboratory (MS-CELL), Center for Natural and Human Sciences, Federal University of ABC, UFABC, Av. dos Estados 5001–Bangú, Santo André 09280-560, SP, Brazil
[4] Grain and Food Science Department, Kansas State University, Manhattan, KS 66506, USA
[5] School of Food Engineering, University of Campinas (UNICAMP), R. Monteiro Lobato 80, Campinas 13083-862, SP, Brazil
* Correspondence: lchani@unaat.edu.pe or larry.76728@gmail.com

Abstract

Chamomile flowers are established in the industry due to their therapeutic characteristics. The leaves are an underused fraction of chamomile production that contains phytochemicals with bioactive properties. This work investigated the extraction of chamomile leaves with supercritical CO_2 (SC-CO_2). The effect of supercritical extraction conditions was evaluated on extraction yield, and the mass transfer process was analyzed by modeling the overall extraction curve (OEC) with empirical and mass balance-based models. Gas chromatography coupled with a mass spectrometer (GC-MS) was used to determine the volatile compounds of the extract. The highest extract yield (1.52 ± 0.01%) was obtained at 300 bar and 45 °C, although similar yields were obtained under conditions of 200 bar/45 °C, 200 bar/35 °C, and 350 bar/35 °C. The 2-straight-line spline promoted the best adjustment to the OEC and described convection as the dominant mass transfer mechanism. The compounds (Z)-2-(Hexa-2,4-diyn-1-ylidene)-1,6-dioxaspiro[4.4]non-3-ene, 2H-1-Benzopyran-2-one,7-methoxy-, cis-beta-Farnesene, alpha-Farnesene, phytol, and (E)-2-(Hepta-2,4-diyn-1-ylidene)-1,6-dioxaspiro[4.4]non-3-ene were the most abundant in the chamomile leaves extracts. SFE extract from chamomile leaves is a promising source of phytochemicals for producing functional products.

Keywords: agro-industrial by-products; chamomile leaves essential oil; extraction kinetics; mathematical modeling; supercritical fluid extraction

Check for updates

Academic Editor: Dariusz Dziki

Received: 8 February 2026
Revised: 1 March 2026
Accepted: 10 March 2026
Published: 16 March 2026

Copyright: © 2026 by the authors. Licensee MDPI, Basel, Switzerland. This article is an open access article distributed under the terms and conditions of the Creative Commons Attribution (CC BY) license.

1. Introduction

Chamomile is a commercial aromatic species cultivated in several countries worldwide [1]. In Peru, the province of Tarma is one of the main chamomile-producing regions, with an estimated 100 ha/year planted, according to the local public agricultural agency [2], probably playing an important role in supplying raw materials for tea production. The weight of fresh chamomile plants ranged from 37.46 to 93.21 g/plant depending on fertilization conditions in a study conducted in Iran by Hadi et al. [3]. The chamomile cultivar

'Złoty Łan' produced approximately 18 inflorescences per plant, and the dry weight of the flower heads per plant was 0.58 g [4]. Chamomile tea is produced exclusively from dried flowers, which confer the characteristic sensory attributes of the infusion [5] and its beneficial health properties [6]. The inclusion of other plant parts in tea production reduces its commercial value [2]. Consequently, chamomile leaves and stems are considered by-products of tea processing, highlighting studies focused on their valorization in order to enhance processing efficiency, sustainability footprint, and overall product quality.

Different parts of the chamomile plant have been reported as sources of bioactive compounds, such as the flowers [7–12], roots [13], leaves [14], and seeds of chamomile [15]. Recent studies highlight chamomile with potential for multiple applications. In the health sector, it has the potential to prevent radiodermatitis [16], reduce oral infections [17], improve childbirth [18], support tumor therapy [19], alleviate depression [20], and exhibit antiosteoporotic effects [21]. In agro-industrial applications, chamomile has been investigated as a feed additive for rabbits [22], an antifungal for crop plants [23], an antiparasitic treatment in poultry [24], and a natural herbicide [25]. Other potential applications reported in the literature include the production of active packaging [26], fermented beverages [27], aromatherapy oil [28], antioxidant sources for functional foods [14], and functional fermented extracts [29]. On the other hand, although the use of the entire chamomile plant negatively affects the commercial value of the tea [2], it has been reported that the leaves contain bioactive compounds of high biological value, such as coumarins (herniarin) [30] and phenolics (mainly rosmarinic acid and quercetin) [14]. Exploring the valorization of chamomile leaves through the extraction of their phytochemicals would contribute to the circular economy of the chamomile tea industry.

Hydrodistillation and supercritical fluid extraction (SFE) have been reported as effective methodologies for obtaining bioactive compounds from chamomile, producing essential oil [7,8] and extracts [12], respectively. When comparing the total extraction yields of the two methods, SFE has a higher yield [9,10]. However, direct comparison between these methods is not appropriate, as hydrodistillation allows obtaining only the volatile fraction, whereas SFE enables the recovery of a broader spectrum of phytochemicals that include volatile and non-volatile compounds.

To the best of the authors' knowledge, limited works have explored the valorization of chamomile leaves—a by-product of tea processing—using supercritical fluid technology. Accordingly, the objective of the research was to evaluate the extraction of chamomile leaves using supercritical CO_2. Specifically, the effects of processing conditions on extraction yield, mathematical modeling, and composition by GC-MS were investigated.

2. Materials and Methods

2.1. Sample Preparation

Five kilograms of chamomile plants were purchased from a local producer in the city of Tarma (Peru). The city has a climate considered temperate and arid, located at 3051 m above sea level, with annual maximum and minimum temperatures of 19.3 and 6.3 °C [31]. The local producer used *Matricaria recutita* seeds (quadrisem, Lot: 617/S4, Italy) supplied by the import company "Manrique" Import Asociados S.R.L., located in the same city. The leaves and flowers were separated manually with the aid of scissors and dried separately at room temperature in the shade. The drying process lasted approximately 9 days; a brittle texture was used as an indicator of proper drying. Drying in the shade at room temperature was selected, as it allows higher essential oil yields, as reported in research with *Stachys lavandulifolia* [32]. After drying, the samples were stored at −20 °C in a laboratory freezer (Meling Biomedical, DW-YL270, Hefei, China) until extraction

experiments. Before extraction experiments by SFE, the samples were ground for 60 s in a homemade immersion blender (Oster, FPSTHB460A-053, 400 W, China).

2.2. Supercritical Fluid Extraction

2.2.1. Extraction Equipment and Extraction Procedure

The extractions were performed in a laboratory SFE unit (Singularity Extraction Technologies, PD-Basic-2235, Campinas, Brazil) with a 100 mL extraction vessel with an inner diameter of 31.38 mm. Twenty grams of sample were placed into the extraction vessel between two layers of glass wool (Dinâmica, CAS: 65997-17-3, Brazil). The bed height for the extractions was 63 mm. The void volume of the extraction vessel was completed with glass beads (3.5–4 mm diameter, ISOLAB Laborgerate GmbH, Carsalo, Brazil). Analytical grade carbon dioxide (Linde Peru S.R.L, 99% pure, Lima, Peru) was used under different thermodynamic conditions to evaluate extraction with different CO_2 densities: 812.69 kg/m^3 (45 °C and 200 bar), 857.14 kg/m^3 (45 °C and 250 bar), 865.72 kg/m^3 (35 °C and 200 bar), 890.33 kg/m^3 (45 °C and 300 bar), 901.23 kg/m^3 (35 °C and 250 bar), 917.12 kg/m^3 (45 °C and 350 bar), 929.11 kg/m^3 (35 °C and 300 bar), and 952.29 kg/m^3 (35 °C and 350 bar) kg/m^3, data obtained from the NIST website [33]. The other operating conditions remained constant, such as mass flow (5.00 g CO_2/min), static time (10 min), and solvent/feed ratio (12.1, g/g). Additionally, chamomile flower extract was prepared under the optimal thermodynamic conditions (200 bar and 40 °C) proposed by Povh et al. [11] to compare its composition with that of the leaves extracts. The micrometering valve was kept at 65 °C during all extractions. Extraction assays were performed in duplicate, and the extracts were stored at approximately −20 °C. The extraction conditions for this study were selected based on studies conducted with chamomile flowers [10–12]. The yield was calculated using Equation (1).

$$X_0 = \frac{m_{EXT}}{F_0} \times 100 \quad (1)$$

where X_0 (%, g/100 g) is the yield, m_{EXT} (g) is the quantity of extract, and F_0 (g) is the amount of raw material inserted in the extraction vessel.

The piping and valve system of the extraction unit (Figure 1) was cleaned after each extraction using a solution of water and ethanol in a ratio of 1:2 (v/v). During cleaning, the micrometering valve was left fully open and heated to 80 °C. Finally, the pipes were dried with a flow of CO_2.

2.2.2. Extraction Kinetics

The OEC was performed under the thermodynamic conditions that provided the best extract yield in the experiments conducted in Section 2.2.1. The extractions were carried out using 29.13 ± 0.08 g of ground dried leaves, which were introduced into the extraction vessel between two layers of glass wool. A constant mass flow rate of solvent (5.00 g CO_2/min) and static time (10 min) were used for the extractions. During the dynamic extraction, the extracts were collected at different times up to approximately 3 h and an S/F of 32.8, to exhaust the extract from the sample. The OEC was plotted with the cumulative yield versus extraction time.

2.3. Mathematical Modeling

In this research, the OEC of chamomile was fitted using a 2-straight-line spline, a logistic model, and desorption-based models.

For the spline model [34] expressed by Equations (2a) and (2b), the adjustable parameters were calculated:

b_0 (g), the linear coefficient;

b_1 (or M_{CER}, in g/min), the mass transfer rate during the constant extraction rate (CER) period;

b_2 (or M_{FER}, in g/min), the mass transfer rate during the falling extraction rate (FER) period; t_{CER} (min), the time-span for the constant extraction rate (CER) period.

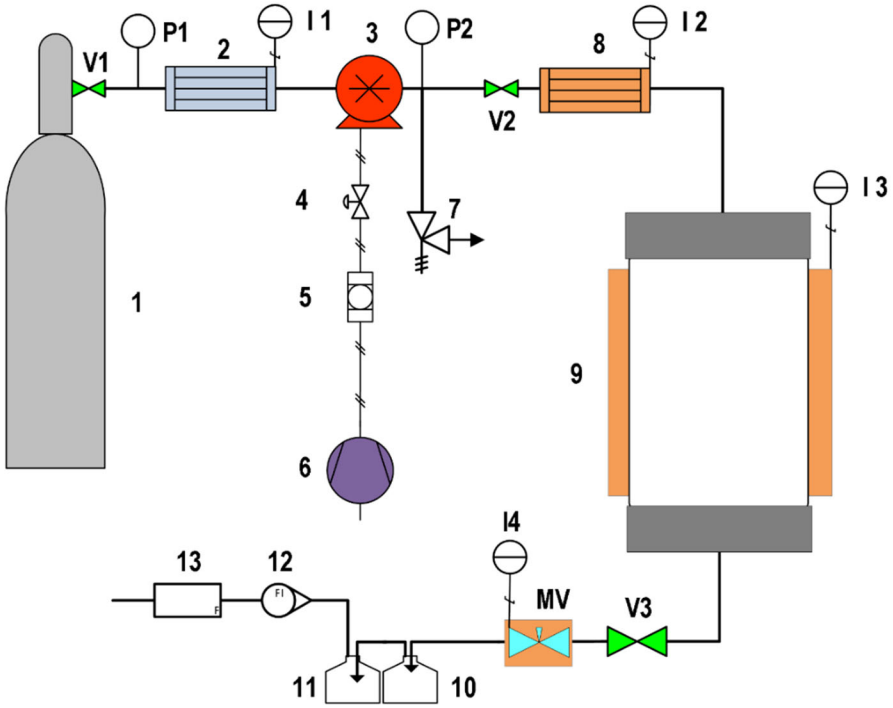


Figure 1. Diagram of the SFE unit (Singularity Extraction Technologies) where V1–V3: blocking valves, P1–P2: Pressure gauge, I1–I4: temperature controllers, MV: micrometric valve, 1: liquid CO_2 cylinder, 2: cooling bath, 3: pneumatic CO_2 pump, 4: compressed air controller, 5: particle filter, 6: air compressor, 7: safety valve, 8: preheater, 9: extraction vessel with heating, 10: extract collector, 11: separator, 12: rotameter, and 13: totalizer.

Subsequently, the parameter Y_{CER} (g extract/g CO_2), defined as the mass ratio of extract in the supercritical phase at the vessel outlet, was calculated as the ratio between b_1 (M_{CER}) and the CO_2 mass flow rate. In addition, the amount of extract recovered during the CER period (R_{CER}, g extract/100 g raw material) was calculated as the ratio between the extraction yield at t_{CER} and the F_0 (g).

When $t \leq t_{CER}$:

$$m_{EXT} = b_0 + b_1 t \tag{2a}$$

When $t_{CER} < t \leq t_{FER}$:

$$m_{EXT} = b_0 + b_1 t + b_2 (t - t_{CER}) \tag{2b}$$

The logistic model [35]—presented in Equation (3)—describes the mass transfer rate using a logistic equation of population growth.

$$m_{EXT} = \frac{X_0 F_0}{\exp(bt_m)} \left\{ \frac{1 + \exp(bt_m)}{1 + [\exp b(t_m - 1)]} - 1 \right\} \tag{3}$$

where m_{EXT} is the amount of extract obtained (g), X_0 is the global yield (g/100 g), F_0 is the amount of raw material used (g), t is the extraction time (min) b is the mass transfer coefficient in the fluid phase (m^{-1}), and t_m (min) is the time associated with the maximum extraction rate.

The amount of extract (g) described by the Tan and Liou [36] model was calculated as shown in Equations (4)–(6):

$$m_{EXT} = \frac{A}{k_d}[1 - exp(k_d B)][exp(-k_d t) - 1] \quad (4)$$

$$A = Q_{CO_2}\frac{1-\varepsilon}{\varepsilon}X_0\frac{\rho_{SAMPLE}}{\rho_{CO2}} \quad (5)$$

$$B = \frac{\varepsilon H}{u} \quad (6)$$

where m_{EXT} (g) is the amount of extract; k_d (min^{-1}) is desorption rate constant which is the adjustable parameter; Q_{CO2} is the CO_2 flow rate; X_0 is the global yield (g/100 g); ε is the bed porosity (-); H is the vessel height (m); ρ_{SAMPLE} and ρ_{CO2} are the densities of sample (kg/m^3) and CO_2 (kg/m^3), respectively; and u is the solvent velocity (m/min).

The model treats solute desorption as a first-order kinetic process, where the extraction rate is proportional to the extracted amount.

The precision of the model in predicting experimental data accurately can decrease under certain operating conditions. Specifically, a relatively high CO_2 flow rate—which may lead to decreased contact time between solute and solvent—and low solute concentration in the supercritical solvent may reduce model accuracy to describe the OEC [37]. Previously, Povh et al. performed SFE of chamomile flowers at 4 g/min [11]. Additionally, the Tan and Liou model was considered not appropriate by Coelho et al. [38].

The model proposed by Goto et al. [39] considers the mass transfer controlled by the desorption mechanism characterized by the attainment of an instantaneous equilibrium. For this model, the overall mass transfer coefficient (ϕ, dimensionless) and the desorption equilibrium constant (k, dimensionless) were calculated.

$$m = \frac{A[\beta/K + (1-\beta)]X_0\rho_s Q_{CO_2}}{\rho}\left\{\frac{\tau}{a_1}\left[exp\left(a_1\frac{t}{\tau}\right) - 1\right] + \frac{\tau}{a_2}\left[1 - exp\left(a_2\frac{t}{\tau}\right)\right]\right\} \quad (7)$$

where

ϕ is the overall mass transfer coefficient (-); k is the desorption equilibrium constant (-); ε is the bed porosity (-); ε_P is the particle porosity of 0.54 [39]; Q_{CO2} is CO_2 flow rate (g/min); τ is CO_2 residence time (min); ρ_S the sample density (g/mL); and a_1, a_2 are the model parameters, expressed by the equations below:

$$a_1 = \frac{1}{2}\left(-b + \sqrt{b^2 - 4c}\right) \quad (8)$$

$$a_2 = \frac{1}{2}\left(-b - \sqrt{b^2 - 4c}\right) \quad (9)$$

$$A = \frac{(1-\varepsilon)\varphi}{[\beta + (1-\beta)K]\varepsilon(a_1 - a_2)} \quad (10)$$

$$b = \frac{\varphi}{[\beta + (1-\beta)K]} + \frac{1}{\varepsilon} + \frac{\varphi(1-\varepsilon)}{\varepsilon} \quad (11)$$

$$c = \frac{\varphi}{[\beta + (1-\beta)K]\varepsilon} \quad (12)$$

$$\varphi = k_p a_p \tau \quad (13)$$

The Solver add-in in Microsoft Excel with the GRG Nonlinear method to minimize the residual sum of squares was used to model the curves.

The effectiveness of each model to describe the kinetics was estimated by calculating the correlation factor (R^2) and the average absolute relative deviation (AARD, %), as described below:

$$AARD(\%) = \frac{1}{n}\sum_{i=1}^{n}\left|\frac{(y_{EXP} - y_P)}{(y_{EXP})}\right| \times 100 \quad (14)$$

where y_{EXP} is the extract yield (%) obtained experimentally, and y_P is the extract yield (%) predicted by the model.

2.4. Composition Analysis

2.4.1. Preparation of Standard and SFE Extract Samples

A homologous series of C8–C20 n-alkane standard and supercritical fluid extraction (SFE) samples obtained from chamomile flowers and leaves under different extraction conditions (200 bar/35 °C, 300 bar/45 °C, and 350 bar/45 °C) were prepared independently prior to GC-MS analysis.

The n-alkane standard mixture was diluted in ethyl acetate at a volumetric ratio of 1:3 (v/v).

For the SFE samples, 0.02 g of each extract was precisely weighed and reconstituted in 2 mL of cyclohexane. The solutions were vortex-mixed to ensure complete dissolution and subsequently centrifuged at 5000 rpm for 5 min to remove any insoluble material. The clear supernatant was carefully collected, and 1.5 mL was filtered through a 0.22 µm PTFE membrane filter into amber glass vials to minimize potential photodegradation prior to chromatographic analysis.

2.4.2. GC-MS Analysis

The volatile constituents of the SFE extracts were characterized using gas chromatography–mass spectrometry (GC–MS) on an Agilent model 7890B GC system coupled to an MSD 5977B quadrupole mass selective detector. Chromatographic separation was performed on a DB-5MS UI capillary column (60 m × 0.25 mm × 1.0 µm film thickness) with helium employed as the carrier gas at a constant flow rate of 1 mL/min.

Samples (1 µL) were injected in split mode (50:1). The injector and transfer line temperatures were maintained at 250 °C and 280 °C, respectively. The oven temperature program was initiated at 60 °C, held for 6 min, followed by a linear ramp of 3 °C/min to 270 °C, with a final hold of 4 min.

Electron impact ionization was performed at 70 eV, with the ion source temperature set at 230 °C and the electron multiplier voltage at 900 V. Mass spectra were acquired in full scan mode over a mass-to-charge (m/z) range of 45 to 450. Compound identification was primarily achieved by comparison of the acquired mass spectra with those in the National Institute of Standards and Technology (NIST 17) mass spectral library [40]. Linear retention indices (LRIs) were calculated using a homologous series of C8–C20 n-alkanes analyzed under identical chromatographic conditions and compared with literature LRI values to support the tentative identification of the detected compounds.

2.5. Statistical Analysis

The experimental data were subjected to Levene's test, Shapiro–Wilk normality test, two-way ANOVA, and Tukey's test using R software (version 4.5.2).

3. Results and Discussion

3.1. SFE Processing

Figure 2 shows the chamomile plant and the residue (leaves) conditioned for the SFE process. Shade-drying the chamomile leaves apparently maintained their green color.

According to the review of the scientific literature conducted by Thamkaew et al. [41], the importance of drying conditions in preserving the quality of aromatic plants is highlighted, with coloration being one of the most important aspects reported in various investigations. The SFE extract of chamomile leaves presented a dark amber color with a characteristic aroma of this plant (Figure 2C).

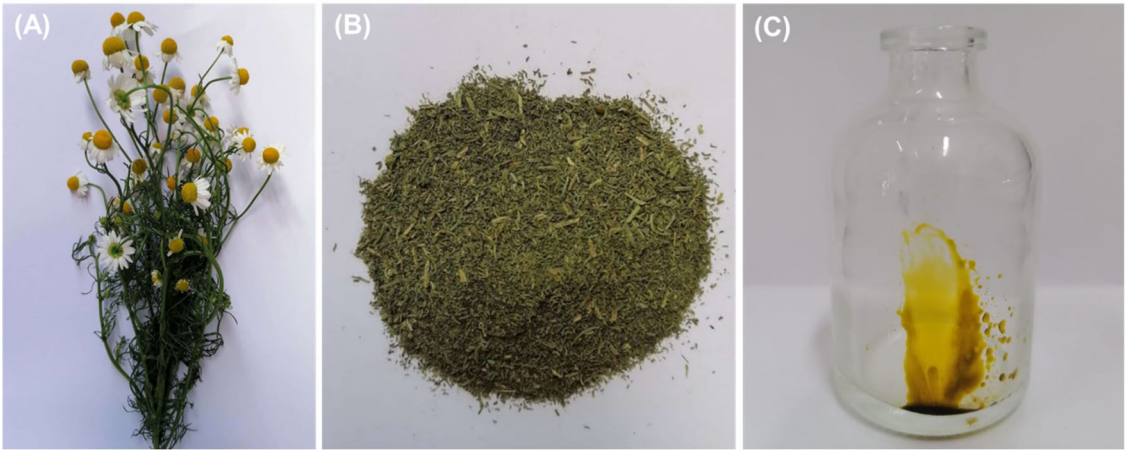


Figure 2. Chamomile plant (**A**), ground dried leaves (**B**), and extract SFE (**C**).

ANOVA showed that temperature as an individual factor did not significantly influence extraction yield, but when interacting with pressure, pressure as an individual factor significantly influenced extract yield (Table 1). Figure 3 presents the global yield of SC-CO_2 extractions obtained for the studied conditions. At both the temperatures studied, extraction yield suffered oscillations with pressure increasing, as it was observed previously for the SC-CO_2 extraction of chamomile flowers at 30–40 °C, 100–200 bar and 1.67 × 10^{-5} kg/s (equivalent to 1.002 g/min) [11]. For example, as observed at 45 °C, the yield decreased from 200 bar (1.48 ± 0.05%) to 250 bar (1.23 ± 0.12%), while from 300 bar (1.52 ± 0.01%) to 350 bar (1.22 ± 0.07%) the yields were slightly lower. At 35 °C, the yield increased from 250 bar to 300 bar because the process overcame the crossover region—between 250 and 300 bar—which is the reverse relationship between temperature and extract solubility [42].

Table 1. Two-way ANOVA from the SFE of chamomile leaves.

Source	Degree Freedom	F-Value	Pr (>F)	
Intercept	1	1173.8121	5.747 × 10^{-10}	***
Pressure (bar)	3	6.3154	0.01669	*
Temperature (°C)	1	0.6311	0.44987	
Pressure × Temperature	3	4.3779	0.04215	*
Residuals	8			

0 (***), 0.01 (*).

At 35 °C, extractions above the crossover pressure of 250 bar increased the yield to 1.35 ± 0.11% (at 300 bar) and 1.45 ± 0.02% (350 bar) The decrease in extraction yield with increasing pressure was also reported by Rahimi et al. [12], who performed SC-CO_2 extraction of chamomile flowers at 30 °C after the pressure increased from 100 to 120 bar, and by Paucarchuco-Soto et al. [42], who performed extraction of *Schinus molle* leaves at 45 °C, where the yield decreased with increasing pressure from 150 to 250 bar. In contrast, the extract yield from *Acacia dealbata* Link. leaves increased when the pressure increased from 200 to 300 bar at 60 °C [43]. The global yield obtained is lower than the findings of Povh et al. [11], who obtained yields ranging between 3.31 and 4.33 g/100 g, from SC-CO_2

extraction of chamomile flowers at the flow rate equivalent to 4 g/min, at 30–40 °C and pressures of 100–200 bar.

Lastly, as is evident, the yield obtained at 200 bar and 45 °C is statistically similar to that obtained at 300 bar and 45 °C. This suggests that the lower pressure extraction condition would be the most suitable for the extraction of chamomile leaves.

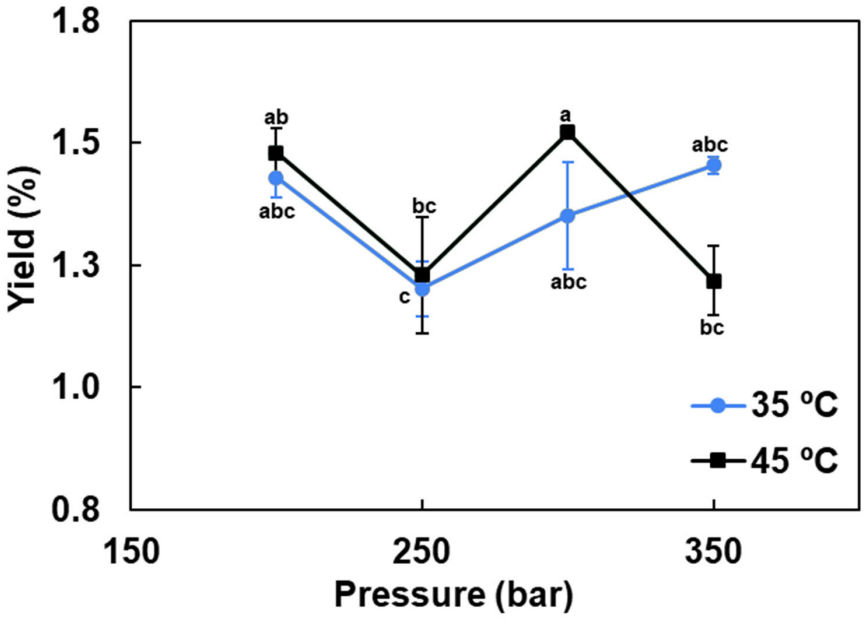


Figure 3. Yields of chamomile leaves extract at different supercritical CO_2 conditions. Values with different letters indicate a significant difference at the 0.05 level.

3.2. OEC Modeling

The experimental and modeled curves are available in Figure 4, and the adjustable parameters are included in Table 2. The analysis of the AARD and R^2 calculated for the models studied (Table 3) indicated that the Spline provided the best adjustment.

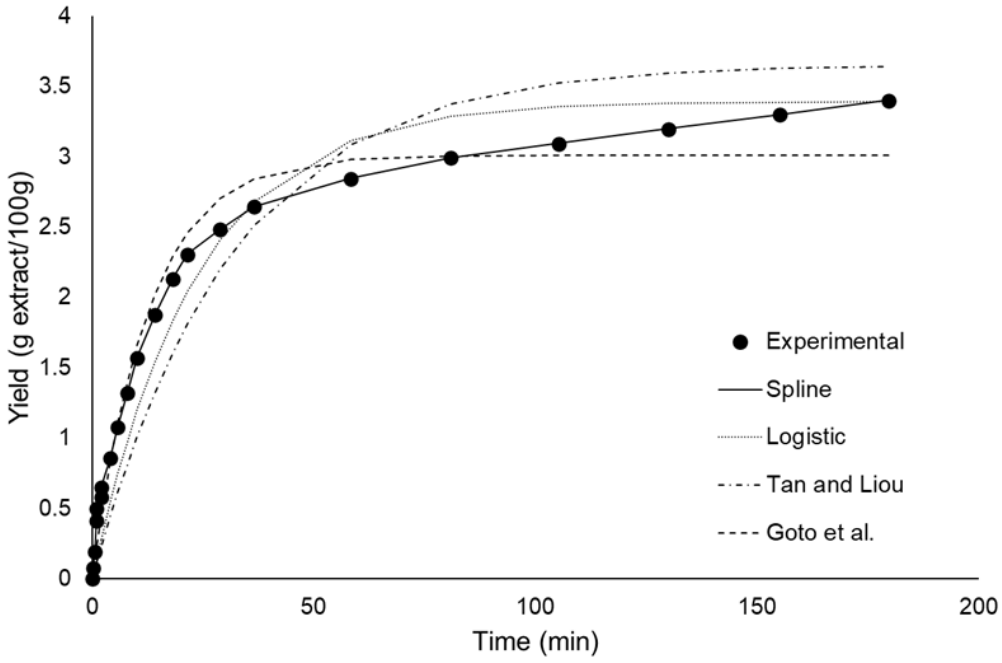


Figure 4. The experimental and modeled OEC of chamomile leaves. The OEC was obtained at the optimal conditions of 200 bar and 35 °C [34–36,39].

Table 2. Adjustable parameters for the modeled OEC of chamomile.

Models	Parameters	Values
Spline [34]	b_0 (g)	2.444×10^{-3}
	$b_1 = M_{CER}$ (g/min)	6.784×10^{-3}
	$b_2 = M_{FER}$ (g/min)	-6.412×10^{-3}
	t_{CER} (min)	17
	R_{CER} (%, g/100 g raw material)	2.135
	Y_{CER} (g extract/g CO_2)	6.784×10^{-3}
Logistic [35]	b (min^{-1})	2.576
	t_m (min)	−10.400
Tan and Liou [36]	k_d (min^{-1})	0.032
Goto et al. [39]	k (-)	0.089
	φ (-)	1.069×10^6

Table 3. The correlation factor and the AARD estimated for the modeled OEC results.

	Spline [34]	Logistic [35]	Tan and Liou [36]	Goto et al. [39]
R^2	0.999	0.99	0.978	0.990
AARD (%)	0.113	29.800	36.652	15.643

Despite the relatively high R^2, the logistic model's AARD was 29.8%, i.e., the predicted data deviated by approximately 30% from the experimental values, and for this reason, did not accurately describe the OECs.

As shown in Figure 4, the chamomile OEC exhibits two periods: (1) the mass transfer occurring in the initial linear portion (CER period: 0–17 min), which is governed by convection between raw material surface and the fluid phase; and (2) the subsequent linear portion (FER period: 17–180 min), during which both convection and diffusion take place. The calculated duration for the CER period (17 min) indicates that more than 60% of the extract was obtained within this stage (Figure 4, Table 2).

No physical meaning was associated with the parameter b (min^{-1}) of the logistic model. However, for the parameter t_m (min)—the time in which the extraction rate reaches its maximum value—a negative value of −10.40 min was calculated, and for this reason, no physical meaning can be attributed to that parameter, similarly to what was found by Bensebia et al. [44], and by Jesus et al. [45].

The desorption constant (k_d, min^{-1}) from the Tan and Liou model [36] represents the rate at which the adsorbed extract is released from the raw material surface into the supercritical solvent. The low k_d value found in this study (0.032 min^{-1}, in Table 2) indicates slower release of extract, possibly due to mass transfer resistance resulting from stronger binding to the raw material. Similar k_d values and lower adjustment performance were also found in the SC-CO_2 extraction of papaya seeds [46].

Originally, the Goto et al. model described the extraction of peppermint oil in supercritical carbon dioxide as a desorption favored by thermodynamic equilibrium due to the raw material fragmentation into different slab elements. As a result, the extract available in the solid phase is transferred to the supercritical fluid, already interacting with the pores of the raw material, which is readily transported. In this work, the Goto et al. [39] model promoted a better response on the OEC modeling—compared to the model of Tan and Liou [36]—because it considers intra-particle diffusion and external mass transfer in the SFE [47].

3.3. Composition of SFE Extract

To the best of the authors' knowledge, works on the chemical composition of chamomile leaves obtained from supercritical fluid extraction are scarce. We also analyzed the SFE extract of chamomile flower (obtained at 200 bar/40 °C) to compare the composition. Table 4 summarizes the volatile compounds identified in the extracts obtained from chamomile leaves and flowers. In addition, Table S1 (supplementary material) provides a comprehensive list of all compounds detected in the extracts, including those not typically associated with chamomile.

Table 4. Abundance (%) of phytochemicals identified in the SFE extract of chamomile leaves and flowers.

RT	Compounds	350 bar/ 45 °C (L)	300 bar/ 45 °C (L)	200 bar/ 35 °C (L)	200 bar/ 40 °C (F)	MF	Formula
23.68	5-Hepten-2-one, 6-methyl-	0.35	0.15	0.15	0.06	98	$C_8H_{14}O$
26.52	o-Cymene	-	-	-	0.01	73	$C_{10}H_{14}$
27.85	1,5-Heptadien-4-one, 3,3,6-trimethyl-	-	-	-	0.07	96	$C_{10}H_{16}O$
29.14	4-Methyl-1,6-heptadien-4-ol	-	-	-	0.01	75	$C_8H_{14}O$
35.76	cis-Ocimenol	-	0.01	-	-	79	$C_{10}H_{18}O$
35.76	trans-Ocimenol	-	0.01	-	-	78	$C_{10}H_{18}O$
35.76	.alpha.-Terpineol	0.01	0.002	-	0.02	71	$C_{10}H_{18}O$
35.97	Naphthalene	-	0.003	-	-	76	$C_{10}H_8$
41.43	1,3,7-Octatriene, 2,7-dimethyl-	-	0.02	-	-	76	$C_{10}H_{16}$
42.60	n-Decanoic acid	-	-	-	0.02	84	$C_{10}H_{20}O_2$
45.05	2,4-Quinolinediol	0.01	0.01	-	-	75	$C_9H_7NO_2$
45.13	Butanoic acid, 3-methyl-, phenylmethyl ester	-	-	-	0.03	90	$C_{12}H_{16}O_2$
45.42	Vanillin	-	0.01	-	-	84	$C_8H_8O_3$
45.42	Benzaldehyde, 2,4-dihydroxy-6-methyl-	-	0.003	-	-	84	$C_8H_8O_3$
47.46	cis-.beta.-Farnesene	15.55	6.66	3.83	8.61	99	$C_{15}H_{24}$
47.96	Coumarin	0.02	0.01	0.01	-	95	$C_9H_6O_2$
48.17	.alpha.-Muurolene	-	0.01	-	-	75	$C_{15}H_{24}$
49.01	trans-.alpha.-Bergamotene	0.15	0.05	0.06	-	96	$C_{15}H_{24}$
49.01	cis-.alpha.-Bergamotene	-	0.33	-	-	97	$C_{15}H_{24}$
49.18	trans-.beta.-Ionone	-	0.04	-	-	75	$C_{13}H_{20}O$
49.69	.alpha.-Farnesene	8.39	6.25	1.60	1.25	98	$C_{15}H_{24}$
49.94	cis-Muurola-4(15),5-diene	0.05	0.02	-	-	84	$C_{15}H_{24}$
49.94	Germacrene D	-	0.07	-	0.24	92	$C_{15}H_{24}$
50.31	.beta.-Bisabolene	0.06	-	0.02	-	76	$C_{15}H_{24}$
52.43	Bicyclo[2.2.1]heptane, 2,2,3-trimethyl-	0.04	0.03	-	-	79	$C_{10}H_{18}$
53.06	(E)-.beta.-Famesene	0.17	-	0.03	-	83	$C_{15}H_{24}$
54.06	1H-Cycloprop[e]azulen-7-ol, decahydro-1,1,7-trimethyl-4-methylene-, [1ar-(1a.alpha.,4a.alpha.,7.beta., 7a.beta.,7b.alpha.)]-	0.57	0.37	0.18	0.09	97	$C_{15}H_{24}O$
54.27	trans-p-mentha-1(7),8-dien-2-ol	0.28	-	-	-	81	$C_{10}H_{16}O$
54.27	(2S,4R)-p-Mentha-[1(7),8]-diene 2-hydroperoxide	0.09	-	-	-	78	$C_{10}H_{16}O_2$
54.36	Farnesene epoxide, E-	0.27	0.07	-	-	83	$C_{15}H_{24}O$
55.23	Trifluoroacetyl-lavandulol	0.01	-	-	-	80	$C_{12}H_{17}F_3O_2$
55.40	Isospathulenol	-	0.09	-	0.14	84	$C_{15}H_{24}O$

Table 4. *Cont.*

RT	Compounds	350 bar/ 45 °C (L)	300 bar/ 45 °C (L)	200 bar/ 35 °C (L)	200 bar/ 40 °C (F)	MF	Formula
55.77	Gossonorol	0.02	0.01	-	0.11	71	$C_{15}H_{22}O$
55.96	Benzophenone	0.04	0.02	0.01	-	90	$C_{13}H_{10}O$
56.49	7-Hydroxyfarnesen	0.77	0.71	0.15	-	93	$C_{15}H_{24}O$
56.84	2-Furanmethanol, tetrahydro-.alpha.,.alpha.,5-trimethyl-5-(4-methyl-3-cyclohexen-1-yl)-, [2S-[2.alpha.,5.beta.(R*)]]-	0.34	0.11	-	0.17	84	$C_{15}H_{26}O_2$
57.10	Xanthoxylin	0.60	0.36	0.08	5.45	94	$C_{10}H_{12}O_4$
57.67	.alpha.-Bisabolol	-	-	-	0.11	92	$C_{15}H_{26}O$
59.18	2H-1-Benzopyran-2-one, 7-methoxy-	18.60	11.13	7.33	2.41	72	$C_{10}H_8O_3$
60.29	Ledol	0.14	-	-	-	81	$C_{15}H_{26}O$
60.66	.alpha.-Phellandrene	-	0.01	-	-	71	$C_{10}H_{16}$
65.10	(Z)-2-(Hexa-2,4-diyn-1-ylidene)-1,6-dioxaspiro [4.4]non-3-ene	33.07	37.24	34.72	34.73	95	$C_{13}H_{12}O_2$
66.32	(E)-2-(Hepta-2,4-diyn-1-ylidene)-1,6-dioxaspiro [4.4]non-3-ene	2.64	1.62	0.15	0.36	89	$C_{14}H_{14}O_2$
71.89	Phytol	7.56	5.44	1.99	0.44	98	$C_{20}H_{40}O$
72.76	9,12,15-Octadecatrienoic acid, (Z,Z,Z)-	1.01	0.64	-	-	83	$C_{18}H_{30}O_2$
73.23	Citronellol	-	-	0.08	-	77	$C_{10}H_{20}O$
73.24	Neophytadiene	0.17	0.08	-	-	84	$C_{20}H_{38}$

RT: Retention time, MF: Match factor, L: Leaves, F: Flower.

(Z)-2-(Hexa-2,4-diyn-1-ylidene)-1,6-dioxaspiro[4.4]non-3-ene is the major constituent in the extracts (Table 4), also known as (Z)-Tonghaosu [48]. Rahimi et al. [12] reported the compound en-in-dicycloether (27.82%) as the major constituent of the SFE extract of chamomile flower. On the other hand, in chamomile flower essential oil, (Z)-Tonghaosu was one of the main components, with a percentage ranging from 10 to 18.7%, depending on the drying method [49].

Two isomers of Farnesene were detected in all the extracts, with a higher abundance of cis-.beta.-Farnesene (3.83–15.55%) followed by alpha.-Farnesene (1.25–8.39%). Cis-beta-farnesene was also reported as one of the most abundant compounds (7.98%) in the supercritical extract of chamomile flowers by Rahimi et al. [12]. In the study conducted by Povh et al. [11], both isomers (alpha and beta) were reported, with beta-farnesene being the most abundant of the two. On the other hand, essential oils obtained from chamomile flowers were found to have a high content of beta-farnesene E (ranging from 15.9 to 25.5%, depending on drying), reported by Benković-Lačić et al. [50], and both isomers (29.8% β-farnesene and 9.3% α-farnesene), reported by Stanojevic et al. [51].

The other major compounds, such as (E)-Tonghaosu, were found in the essential oil of *Matricaria chamomilla* [52] and extracts of *Chenopodium ambrosioides* (leaves and stems) [53]. Phytol was found in the trans configuration in the essential oil of *M. chamomilla*, but in lower abundance (3.28%) compared to the essential oil of *Morus nigra* [54]. 2H-1-Benzopyran-2-one, 7-methoxy-, known as 7-Methoxycoumarin [55], was reported in lower abundance (1.09%) in the SFE extract of chamomile flower reported by Rahimi et al. [12] compared to the results of the present study (Table 4), which ranged from 2.41 to 18.60%, with the lowest being for the chamomile flower extract. An interesting content of 7-Methoxycoumarin (82.79 mg/100 g) was also reported in the extracts obtained by maceration from chamomile processing residues [56].

The abundant biomolecules in chamomile leaves exhibit diverse biological properties (Table 4). Beta-farnesene exhibits a repellent effect and a synergistic effect with different

insecticides against agricultural pests, such as *Myzus persicae* [57], and a synergistic effect against *Lipaphis erysimi* [58]. In addition, there are toxic effects against larvae of agricultural pests such as *Spodoptera litura* with an LC_{50} of 16.13 µg/mL, *Helicoverpa armigera* with an LC_{50} of 15.50 µg/mL, and against larvae of the vectors *Aedes vittatus* with an LC_{50} of 5.66 µg/mL, and *Anopheles subpictus* with an LC_{50} of 6.08 µg/mL [59].

(E)-Tonghaosu and its analogues showed antifeedant activity against the larvae of the agricultural pest *Pieris brassicae* [60], and other biological activities (regulating metabolism, immune cell balance, and type II diabetes mellitus) for applications in medicine [61]. On the other hand, phytol has potential use in the pharmaceutical industry, presenting anxiolytic, cytotoxic, antioxidant, autophagy and apoptosis-inducing, antinociceptive, immunomodulatory, antimicrobial [62], antihyperalgesic, anti-inflammatory, and antiarthritic properties [63].

4. Conclusions

As by-products of the tea-processing chain, chamomile leaves were hypothesized as a potential source of bioactive compounds. The bioactive compounds from chamomile leaves were optimally extracted with supercritical CO_2 under moderate operating conditions (200 bar, 35 °C and 5.00 g of CO_2/min), obtaining a yield of 3.40 g of extract per 100 g of sample after a processing time of 179.5 min and an S/F ratio of 32.9. Despite its empirical nature, the 2-line-spline model provided the best adjustment to the experimental data, and an approximate description of the mass transfer mechanisms in the SFE occur in the form of convection (first part of the curve) and convection + diffusion (second part of the OEC). Interestingly, less than 70% of the extract was obtained in the CER period, indicating lower extract release, which is confirmed by the low values calculated for the desorption rate k_d of the Tan and Liou model, and for the desorption equilibrium constant k' of the Goto et al. model. The extracts analyzed are rich in (Z)-2-(Hexa-2,4-diyn-1-ylidene)-1,6-dioxaspiro[4.4]non-3-ene, 2H-1-Benzopyran-2-one,7-methoxy-, cis-beta-Farnesene, alpha-Farnesene, phytol, and (E)-2-(Hepta-2,4-diyn-1-ylidene)-1,6-dioxaspiro[4.4]non-3-ene. The SFE extracts obtained in this work consist of a complex mixture of phytochemicals that could support its use in industry, requiring further studies for the fractionation, purification, and evaluation of the biological properties of the most valuable phytochemicals in chamomile leaves.

Supplementary Materials: The following supporting information can be downloaded at: https://www.mdpi.com/article/10.3390/pr14060942/s1, Table S1. Results of GC-MS analysis of SFE extracts from chamomile leaves and flowers.

Author Contributions: Conceptualization, L.O.C.-P.; methodology, J.P.-S., D.M.-M., G.W.Q.S., P.C.-R., J.C.M.S., J.C.J.F. and Á.L.S.; formal analysis, L.O.C.-P.; investigation, L.O.C.-P. and M.A.A.M.; resources, L.O.C.-P.; data curation, L.O.C.-P., J.C.M.S. and J.C.J.F.; writing—original draft, L.O.C.-P., D.M.-M., G.W.Q.S., P.C.-R. and J.C.M.S.; writing—review and editing, L.O.C.-P., W.J.C.C., Á.L.S. and M.A.A.M.; project administration, L.O.C.-P.; funding acquisition, L.O.C.-P. All authors have read and agreed to the published version of the manuscript.

Funding: L.O.Chañi-Paucar thanks "UNAAT INVESTIGA" (ficance code "P2-23-01-01"; Vicepresidencia de Investigación of the Universidad Nacional Autónoma Altoandina de Tarma) for the financial support throughout the Science, Technology, and Innovation Project "Valorización de especies vegetales aromáticas comercializadas en la ciudad de Tarma para la obtención de compuestos volátiles usando tecnología de fluidos supercríticos". M.A.A.Meireles thanks CNPq (309825-2020-2).

Data Availability Statement: The original contributions presented in this study are included in the article. Further inquiries can be directed to the corresponding author.

Conflicts of Interest: The authors declare no conflict of interest.

References

1. Parveen, A.; Perveen, S.; Naz, F.; Ahmad, M.; Khalid, M. Chamomile. In *Essentials of Medicinal and Aromatic Crops*; Springer: Cham, Switzerland, 2023; pp. 1009–1040. [CrossRef]
2. Aliaga-Paredes, E.-L.; Acevedo-Jara, J.A. Factores Para El Procesamiento de La Manzanilla Común En La Industria Peruana de Infusiones. *Ing. Ind.* **2018**, *36*, 213–239. [CrossRef]
3. Hadi, M.R.H.S.; Fallah, M.A.; Darzi, M.T. View of Influence of Nitrogen Fertilizer and Vermicompost Application on Flower Yield and Essential Oil of Chamomile (*Matricaria chamomile* L.). *J. Chem. Health Risks* **2015**, *5*, 235–244.
4. Kwiatkowski, C.A.; Harasim, E.; Feledyn-Szewczyk, B.; Stalenga, J.; Jańczak-Pieniążek, M.; Buczek, J.; Nnolim, A. Productivity and Quality of Chamomile (*Chamomilla recutita* (L.) Rausch.) Grown in an Organic System Depending on Foliar Biopreparations and Row Spacing. *Agriculture* **2022**, *12*, 1534. [CrossRef]
5. Yang, J.E.; Lee, J. Consumer Perception and Liking, and Sensory Characteristics of Blended Teas. *Food Sci. Biotechnol.* **2020**, *29*, 63–74. [CrossRef]
6. McKay, D.L.; Blumberg, J.B. A Review of the Bioactivity and Potential Health Benefits of Chamomile Tea (*Matricaria recutita* L.). *Phytother. Res.* **2006**, *20*, 519–530. [CrossRef]
7. Sarma, N.; Gogoi, R.; Begum, T.; Lal, M.; Perveen, K.; Alsahikh, N.A.; Alsulami, J.A. A Study on the Chemical Profile of Cultivated Chamomile (*Matricaria chamomilla* L.) Flower Essential Oil from North East India with Special Emphasis on Its Pharmacological Importance. *J. Essent. Oil Bear. Plants* **2023**, *26*, 745–760. [CrossRef]
8. Alahmady, N.F.; Alkhulaifi, F.M.; Abdullah Momenah, M.; Ali Alharbi, A.; Allohibi, A.; Alsubhi, N.H.; Ahmed Alhazmi, W. Biochemical Characterization of Chamomile Essential Oil: Antioxidant, Antibacterial, Anticancer and Neuroprotective Activity and Potential Treatment for Alzheimer's Disease. *Saudi J. Biol. Sci.* **2024**, *31*, 103912. [CrossRef] [PubMed]
9. Herrera, E.; Pacheco, C.; Olivera-Montenegro, L. Extraction and Characterization of Chamomile (*Matricaria recutita* L.) Essential Oil Using the Green Technology of Solvent-Free Microwave Extraction. *Biol. Life Sci. Forum* **2022**, *18*, 12974. [CrossRef]
10. Kotnik, P.; Škerget, M.; Knez, Ž. Supercritical Fluid Extraction of Chamomile Flower Heads: Comparison with Conventional Extraction, Kinetics and Scale-Up. *J. Supercrit. Fluids* **2007**, *43*, 192–198. [CrossRef]
11. Povh, N.P.; Marques, M.O.M.; Meireles, M.A.A. Supercritical CO_2 Extraction of Essential Oil and Oleoresin from Chamomile (*Chamomilla recutita* [L.] Rauschert). *J. Supercrit. Fluids* **2001**, *21*, 245–256. [CrossRef]
12. Rahimi, E.; Prado, J.M.; Zahedi, G.; Meireles, M.A.A. Chamomile Extraction with Supercritical Carbon Dioxide: Mathematical Modeling and Optimization. *J. Supercrit. Fluids* **2011**, *56*, 80–88. [CrossRef]
13. Mailänder, L.K.; Lorenz, P.; Bitterling, H.; Stintzing, F.C.; Daniels, R.; Kammerer, D.R. Phytochemical Characterization of Chamomile (*Matricaria recutita* L.) Roots and Evaluation of Their Antioxidant and Antibacterial Potential. *Molecules* **2022**, *27*, 8508. [CrossRef]
14. Cho, Y.-J.; Yoon, S.-J.; Kim, J.-H.; Chun, S.-S. Biological Activity of Chamomile (*Matricaria chamomilla* L.) Extracts. *J. Korean Soc. Food Sci. Nutr.* **2005**, *34*, 446–450. [CrossRef]
15. Milovanovic, S.; Grzegorczyk, A.; Świątek, Ł.; Grzęda, A.; Dębczak, A.; Tyskiewicz, K.; Konkol, M. A Novel Strategy for the Separation of Functional Oils from Chamomile Seeds. *Food Bioproc. Technol.* **2023**, *16*, 1806–1821. [CrossRef]
16. Garbuio, D.C.; Ribeiro, V.D.S.; Hamamura, A.C.; Faustino, A.; De Freitas, L.A.P.; Viani, G.; Carvalho, E.C. De A Chitosan-Coated Chamomile Microparticles Formulation to Prevent Radiodermatitis in Breast: A Double-Blinded, Controlled, Randomized, Phase II Clinical Trial. *Am. J. Clin. Oncol. Cancer Clin. Trials* **2022**, *45*, 183–189. [CrossRef]
17. Naghsh, N.; Moghareabed, A.; Nematnejad, M.; Yaghini, J.; Sadeghi, S.M. A Comparative Evaluation of the Antimicrobial Effect of Chamomile, Aloe Vera-Green Tea, and Chlorhexidine Mouthwashes on Some Oral Bacterial Species. *Dent. Res. J.* **2023**, *20*, 70. [CrossRef]
18. Eskandari, F.; Mousavi, P.; Valiani, M.; Ghanbari, S.; Iravani, M. A Comparison of the Effect of Swedish Massage with and without Chamomile Oil on Labor Outcomes and Maternal Satisfaction of the Childbirth Process: A Randomized Controlled Trial. *Eur. J. Med. Res.* **2022**, *27*, 266. [CrossRef]
19. Selim, A.A.; Abdelmonem, I.M.; Amin, M.A.; Essa, B.M. Biogenic Harmony of Biocompatible Silver Nanoplatforms Using Chamomile Extract and Apigenin-7-Glucoside for Solid Tumor Therapy. *J. Radioanal. Nucl. Chem.* **2024**, *333*, 705–715. [CrossRef]
20. Ebrahimi, H.; Mardani, A.; Basirinezhad, M.H.; Hamidzadeh, A.; Eskandari, F. The Effects of Lavender and Chamomile Essential Oil Inhalation Aromatherapy on Depression, Anxiety and Stress in Older Community-Dwelling People: A Randomized Controlled Trial. *Explore* **2022**, *18*, 272–278. [CrossRef] [PubMed]
21. Raja, A.; Singh, G.P.; Fadil, S.A.; Elhady, S.S.; Youssef, F.S.; Ashour, M.L. Prophylactic Anti-Osteoporotic Effect of *Matricaria chamomilla* L. Flower Using Steroid-Induced Osteoporosis in Rat Model and Molecular Modelling Approaches. *Antioxidants* **2022**, *11*, 1316. [CrossRef]
22. Nasr, A.M.; Aboul Ela, S.E.D.S.; Ismail, I.E.; Aldhahrani, A.; Soliman, M.M.; Alotaibi, S.S.; Bassiony, S.S.; Abd El-Hack, M.E. A Comparative Study among Dietary Supplementations of Antibiotic, Grape Seed and Chamomile Oils on Growth Performance and Carcass Properties of Growing Rabbits. *Saudi J. Biol. Sci.* **2022**, *29*, 2483–2488. [CrossRef] [PubMed]

23. Baka, Z.A.M.; El-Sharkawy, A.M.; El-Zahed, M.M. Anti-Aspergillus Niger Action of Biosynthesized Silicon Dioxide Nanoparticles Alone or Combined with *Matricaria chamomilla* L. Extract. *J. Microbiol. Biotechnol. Food Sci.* **2024**, *13*, e10816. [CrossRef]
24. Beski, S.S.M. Anti-Coccidial Effects of Dietary Chamomile against Experimentally Induced Coccidiosis in Broiler Chicken. *Czech J. Anim. Sci.* **2023**, *68*, 30–43. [CrossRef]
25. Madadi, E.; Fallah, S.; Sadeghpour, A.; Barani-Beiranvand, H. Exploring the Use of Chamomile (*Matricaria chamomilla* L.) Bioactive Compounds to Control Flixweed (*Descurainia sophia* L.) in Bread Wheat (*Triticum aestivum* L.): Implication for Reducing Chemical Herbicide Pollution. *Saudi J. Biol. Sci.* **2022**, *29*, 103421. [CrossRef]
26. Sayah, N.; Salem, A.; Abdelhedi, O.; Balti, R.; Zouari, N.; Debeaufort, F.; Hamdi, N.; Jridi, M. Potential of Smectite/Illite/Chamomile Extract in Gelatin Films as Active Food Packaging Materials. *EuroMediterr. J. Environ. Integr.* **2024**, *9*, 1537–1550. [CrossRef]
27. Mascarin, L.G.; Franco, F.W.; Dornelles, R.C.; Figueredo, K.C.; Santos, R.O.; de Freitas Bauermann, L.; Emanuelli, T.; Somacal, S.; Sautter, C.K. Effect of Adding *Matricaria recutita* L., *Cymbopogon citratus*, or *Mentha piperita* L. Extracts to Fermented Orange Beverage: Sensory Evaluation, Physicochemical Characterization, and Prediction of Toxic Risks and Biological Activity In Silico. *Foods* **2023**, *12*, 243. [CrossRef] [PubMed]
28. Ma'arif, B.; Nurfadhilah, E.; Muslikh, F.A.; Aditama, A.P.R.; Suryadinata, A.; Ahdi, I.R.; Taek, M.M.; Maulina, N. Formulation of Aromatherapy Massage Oil from Lavender (*Lavandula angustifolia*), Chamomile (*Matricaria recutit*), and Petitgrain (*Citrus aurantium*) for Stress Relief. *J. Med. Chem. Sci.* **2023**, *6*, 3078–3086. [CrossRef]
29. Mailänder, L.K.; Nosrati Gazafroudi, K.; Greiß, M.; Lorenz, P.; Nicolay, S.; Gründemann, C.; Stintzing, F.C.; Daniels, R.; Kammerer, D.R. Impact of Fermentation on the Phytochemical Profile and Bioactivity Characteristics of Aqueous *Matricaria recutita* L. Root Extracts. *Chem. Biodivers.* **2024**, *21*, e202400159. [CrossRef]
30. Jasim, L.M.M.; Homayouni Tabrizi, M.; Darabi, E.; Jaseem, M.M.M. The Antioxidant, Anti-Angiogenic, and Anticancer Impact of Chitosan-Coated Herniarin-Graphene Oxide Nanoparticles (CHG-NPs). *Heliyon* **2023**, *9*, e20042. [CrossRef]
31. Instituto Geofísico del Perú El Clima En El Perú. Available online: http://met.igp.gob.pe/ (accessed on 25 February 2026).
32. Hazrati, S.; Lotfi, K.; Govahi, M.; Ebadi, M.T. A Comparative Study: Influence of Various Drying Methods on Essential Oil Components and Biological Properties of *Stachys lavandulifolia*. *Food Sci. Nutr.* **2021**, *9*, 2612–2619. [CrossRef]
33. NIST—National Institute of Standards and Technology. Propiedades Termofísicas de Sistemas Fluidos. Available online: https://webbook.nist.gov/chemistry/fluid/ (accessed on 25 February 2026).
34. Meireles, M.A.A. Extraction of Bioactive Compounds from Latin American Plants. In *Supercritical Fluid Extraction of Nutraceuticals and Bioactive Compounds*; Martinez, J., Ed.; CRC Press—Taylor & Francis Group: Boca Raton, FL, USA, 2008; pp. 243–274.
35. Martínez, J.; Monteiro, A.R.; Rosa, P.T.V.; Marques, M.O.M.; Meireles, M.A.A. Multicomponent Model To Describe Extraction of Ginger Oleoresin with Supercritical Carbon Dioxide. *Ind. Eng. Chem. Res.* **2003**, *42*, 1057–1063. [CrossRef]
36. Tan, C.-S.; Liou, D.-C. Modeling of Desorption at Supercritical Conditions. *AIChE J.* **1989**, *35*, 1029–1031. [CrossRef]
37. Banafi, A.; Wee, S.K.; Tiong, A.N.T.; Kong, Z.Y.; Saptoro, A.; Sunarso, J. Modeling of Supercritical Fluid Extraction Bed: A Critical Review. *Chem. Eng. Res. Des.* **2023**, *193*, 685–712. [CrossRef]
38. Coelho, J.P.; Robalo, M.P.; Fernandes, I.S.; Stateva, R.P. Optimization of Oil Recovery from Japonica Luna Rice Bran by Supercritical Carbon Dioxide Applying Design of Experiments: Characterization of the Oil and Mass Transfer Modeling. *ChemEngineering* **2022**, *6*, 63. [CrossRef]
39. Goto, M.; Sato, M.; Hirose, T. Extraction of Peppermint Oil by Supercritical Carbon Dioxide. *J. Chem. Eng. Jpn.* **1993**, *26*, 401–407. [CrossRef]
40. Smeriglio, A.; Alloisio, S.; Raimondo, F.M.; Denaro, M.; Xiao, J.; Cornara, L.; Trombetta, D. Essential Oil of Citrus Lumia Risso: Phytochemical Profile, Antioxidant Properties and Activity on the Central Nervous System. *Food Chem. Toxicol.* **2018**, *119*, 407–416. [CrossRef]
41. Thamkaew, G.; Sjöholm, I.; Galindo, F.G. A Review of Drying Methods for Improving the Quality of Dried Herbs. *Crit. Rev. Food Sci. Nutr.* **2021**, *61*, 1763–1786. [CrossRef] [PubMed]
42. Paucarchuco-Soto, J.; Padilla Pacahuala, G.; Cuadrado Campó, W.J.; Chagua-Rodríguez, P.; Maceda Santivañez, J.C.; Santana, Á.L.; Meireles, M.A.A.; Chañi-Paucar, L.O. Supercritical Fluid Extraction of Peruvian *Schinus molle* Leaves: Yield, Kinetics, Mathematical Modeling, and Chemical Composition. *Processes* **2025**, *13*, 2191. [CrossRef]
43. Rodrigues, V.H.; Portugal, I.; Silva, C.M. Experimental Optimization of the Supercritical Fluid Extraction of Triterpenoids from *Acacia dealbata* Link. *Leaves. Sep. Purif. Technol.* **2023**, *306*, 122637. [CrossRef]
44. Bensebia, O.; Bensebia, B.; Allia, K.; Barth, D. Supercritical CO_2 Extraction of Triterpenes from Rosemary Leaves: Kinetics and Modelling. *Sep. Sci. Technol.* **2016**, *51*, 2174–2182. [CrossRef]
45. Jesus, S.P.; Grimaldi, R.; Hense, H. Recovery of γ-Oryzanol from Rice Bran Oil Byproduct Using Supercritical Fluid Extraction. *J. Supercrit. Fluids* **2010**, *55*, 149–155. [CrossRef]
46. Hall, R.M.; Mayer, D.A.; Mazzutti, S.; Ferreira, S.R.S. Simulating Large Scale SFE Applied to Recover Bioactive Compounds from Papaya Seeds. *J. Supercrit. Fluids* **2018**, *140*, 302–309. [CrossRef]

47. Rai, A.; Punase, K.D.; Mohanty, B.; Bhargava, R. Evaluation of Models for Supercritical Fluid Extraction. *Int. J. Heat Mass Transf.* **2014**, *72*, 274–287. [CrossRef]
48. NIST. (Z)-2-(Hexa-2,4-diyn-1-ylidene)-1,6-dioxaspiro[4.4]non-3-ene. Available online: https://webbook.nist.gov/cgi/cbook.cgi?Name=%28Z%29-2-%28Hexa-2%2C4-diyn-1-ylidene%29-1%2C6-dioxaspiro%5B4.4%5Dnon-3-ene&Units=SI (accessed on 27 January 2026).
49. Abbas, A.M.; Seddik, M.A.; Gahory, A.A.; Salaheldin, S.; Soliman, W.S. Differences in the Aroma Profile of Chamomile (*Matricaria chamomilla* L.) after Different Drying Conditions. *Sustainability* **2021**, *13*, 5083. [CrossRef]
50. Benković-Lačić, T.; Orehovec, I.; Mirosavljević, K.; Benković, R.; Ćavar Zeljković, S.; Štefelová, N.; Tarkowski, P.; Salopek-Sondi, B. Effect of Drying Methods on Chemical Profile of Chamomile (*Matricaria chamomilla* L.) Flowers. *Sustainability* **2023**, *15*, 15373. [CrossRef]
51. Stanojevic, L.P.; Marjanovic-Balaban, Z.R.; Kalaba, V.D.; Stanojevic, J.S.; Cvetkovic, D.J. Chemical Composition, Antioxidant and Antimicrobial Activity of Chamomile Flowers Essential Oil (*Matricaria chamomilla* L.). *J. Essent. Oil-Bear. Plants* **2016**, *19*, 2017–2028. [CrossRef]
52. Zhang, L.; Liang, X.; Wang, B.; Lin, Z.; Ye, M.; Ma, R.; Zheng, M.; Xiang, H.; Xu, P. Six Herbs Essential Oils Suppressing Inflammatory Responses via Inhibiting COX-2/TNF-α/IL-6/NF-KB Activation. *Microchem. J.* **2020**, *156*, 104769. [CrossRef]
53. Abdulkader, O.M.; Sharaf, A.E.A.; Fouda, H.M.; Elhaw, M.H. Phytoconstitutes Investigation of *Chenopodium ambrosioides* Linn. and Gas Chromatography with Mass Spectroscopy Material Analysis. *Mater. Today Proc.* **2022**, *61*, 992–997. [CrossRef]
54. Hajdari, A.; Kelmendi, N.; Mustafa, G.; Mustafa, B.; Nebija, D. Volatile Constituents of Some Selected Plant Species Traditionally Used as Tea in the Sharri Mountains (Kosovo). *Sci. World J.* **2022**, *2022*, 2594195. [CrossRef]
55. NIST. 2H-1-Benzopyran-2-one, 7-Methoxy-. Available online: https://webbook.nist.gov/cgi/cbook.cgi?Name=7-Methoxycoumarin+&Units=SI (accessed on 27 January 2026).
56. Molnar, M.; Mendešević, N.; Šubarić, D.; Banjari, I.; Jokić, S. Comparison of Various Techniques for the Extraction of Umbelliferone and Herniarin in *Matricaria chamomilla* Processing Fractions. *Chem. Cent. J.* **2017**, *11*, 78. [CrossRef]
57. Zhang, Y.; Huang, Y.; Liu, Y.; Li, Z.; Yang, X.; Qin, Y. Synergism of (E)-β-Farnesene and Its Analogue to Insecticides against the Green Peach Aphid *Myzus persicae*. *J. Agric. Food Chem.* **2024**, *72*, 17317–17327. [CrossRef]
58. Cui, L.-L.; Dong, J.; Francis, F.; Liu, Y.-J.; Heuskin, S.; Lognay, G.; Chen, J.-L.; Bragard, C.; Tooker, J.F.; Liu, Y. E-β-Farnesene Synergizes the Influence of an Insecticide to Improve Control of Cabbage Aphids in China. *Crop Prot.* **2012**, *35*, 91–96. [CrossRef]
59. Al-Ghanim, K.A.; Krishnappa, K.; Pandiyan, J.; Nicoletti, M.; Gurunathan, B.; Govindarajan, M. Insecticidal Potential of *Matricaria chamomilla*'s Essential Oil and Its Components (E)-β-Farnesene, Germacrene D, and α-Bisabolol Oxide A against Agricultural Pests, Malaria, and Zika Virus Vectors. *Agriculture* **2023**, *13*, 779. [CrossRef]
60. Chen, L.; Xu, H.-H.; Yin, B.-L.; Xiao, C.; Hu, T.-S.; Wu, Y.-L. Synthesis and Antifeeding Activities of Tonghaosu Analogues. *J. Agric. Food Chem.* **2004**, *52*, 6719–6723. [CrossRef]
61. Zhang, F.; Iwaki, A.; Ishiuchi, K.; Sugiyama, A.; Ohsawa, M.; Makino, T. Peroxisome Proliferator-Activated Receptor-γ Agonistic Effect of *Chrysanthemum indicum* Capitulum and Its Active Ingredients. *Pharmacogn. Mag.* **2018**, *14*, 461. [CrossRef]
62. Islam, M.T.; Ali, E.S.; Uddin, S.J.; Shaw, S.; Islam, M.A.; Ahmed, M.I.; Chandra Shill, M.; Karmakar, U.K.; Yarla, N.S.; Khan, I.N.; et al. Phytol: A Review of Biomedical Activities. *Food Chem. Toxicol.* **2018**, *121*, 82–94. [CrossRef]
63. Carvalho, A.M.S.; Heimfarth, L.; Pereira, E.W.M.; Oliveira, F.S.; Menezes, I.R.A.; Coutinho, H.D.M.; Picot, L.; Antoniolli, A.R.; Quintans, J.S.S.; Quintans-Júnior, L.J. Phytol, a Chlorophyll Component, Produces Antihyperalgesic, Anti-Inflammatory, and Antiarthritic Effects: Possible NFκB Pathway Involvement and Reduced Levels of the Proinflammatory Cytokines TNF-α and IL-6. *J. Nat. Prod.* **2020**, *83*, 1107–1117. [CrossRef] [PubMed]

Disclaimer/Publisher's Note: The statements, opinions and data contained in all publications are solely those of the individual author(s) and contributor(s) and not of MDPI and/or the editor(s). MDPI and/or the editor(s) disclaim responsibility for any injury to people or property resulting from any ideas, methods, instructions or products referred to in the content.